JCI The Journal of Clinical Investigation

IRGM1 supports host defense against intracellular bacteria through suppression of type I interferon in mice

Prashant Rai, … , Gregory A. Taylor, Michael B. Fessler

J Clin Invest. 2023;133(21):e171982. https://doi.org/10.1172/JCI171982.

Research Letter | Immunology | Infectious disease

To the Editor: IFN-γ enhances cell-autonomous host defense by inducing several families of antimicrobial target genes, including immunity-related GTPases (IRGs). Animals deficient in IRGM1, the best-studied IRG, succumb to numerous bacterial and protozoal infections in a manner that nearly phenocopies that of IFN-γ–null mice (1). This infection susceptibility has been attributed to the cell-intrinsic role of IRGM1 in xenophagy and targeting of pathogen-containing vacuoles (1). Recently, we reported that Irgm1-/- mice spontaneously produce excess type I IFN (IFN-I) (2). Although IFN-I is protective against virus, it can compromise antibacterial host defense (3). We hypothesized that IFN-I, rather than defective cell-intrinsic defenses, drives the susceptibility of Irgm1–/– mice to bacteria. Consistent with this, we found that Irgm1–/– mice succumbed to Mycobacterium tuberculosis and Listeria monocytogenes, as previously reported (1), but Irgm1–/– mice lacking the IFN-I receptor, IFNAR1 (i.e., Irgm1–/–Ifnar–/– mice), were resistant (Figure 1A). Similarly, the increased pathogen burden in Irgm1–/– mice following infection with Salmonella typhimurium was normalized in Irgm1–/–Ifnar–/– mice (Figure 1A). By contrast, during infection with Toxoplasma gondii, a pathogen for which IFN-I is host protective (4), Irgm1–/– mice had reduced survival, and this was not rescued in Irgm1–/–Ifnar–/– animals (Supplemental Figure 1A; supplemental material, including the Supplemental Methods, available online with this article; https://doi.org/10.1172/JCI171982DS1). To investigate IFN-I's mechanism of compromising host defense in Irgm1–/– mice, we pursued […]

IRGM1 supports host defense against intracellular bacteria through suppression of type I interferon in mice

To the Editor: IFN-γ enhances cell-autonomous host defense by inducing several families of antimicrobial target genes, including immunity-related GTPases (IRGs). Animals deficient in IRGM1, the best-studied IRG, succumb to numerous bacterial and protozoal infections in a manner that nearly phenocopies that of IFN-γ–null mice (1). This infection susceptibility has been attributed to the cell-intrinsic role of IRGM1 in xenophagy and targeting of pathogen-containing vacuoles (1).

Recently, we reported that *Irgm1*$^{-/-}$ mice spontaneously produce excess type I IFN (IFN-I) (2). Although IFN-I is protective against virus, it can compromise antibacterial host defense (3). We hypothesized that IFN-I, rather than defective cell-intrinsic defenses, drives the susceptibility of *Irgm1*$^{-/-}$ mice to bacteria. Consistent with this, we found that *Irgm1*$^{-/-}$ mice succumbed to *Mycobacterium tuberculosis* and *Listeria monocytogenes*, as previously reported (1), but *Irgm1*$^{-/-}$ mice lacking the IFN-I receptor, IFNAR1 (i.e., *Irgm1*$^{-/-}$*Ifnar*$^{-/-}$ mice), were resistant (Figure 1A). Similarly, the increased pathogen burden in *Irgm1*$^{-/-}$ mice following infection with *Salmonella typhimurium* was normalized in *Irgm1*$^{-/-}$*Ifnar*$^{-/-}$ mice (Figure 1A). By contrast, during infection with *Toxoplasma gondii*, a pathogen for which IFN-I is host protective (4), *Irgm1*$^{-/-}$ mice had reduced survival, and this was not rescued in *Irgm1*$^{-/-}$*Ifnar*$^{-/-}$ animals (Supplemental Figure 1A; supplemental material, including the Supplemental Methods, available online with this article; https://doi.org/10.1172/JCI171982DS1).

To investigate IFN-I's mechanism of compromising host defense in *Irgm1*$^{-/-}$ mice, we pursued the *L. monocytogenes* infection model. After infection, *Irgm1*$^{-/-}$ mice had elevated biomarkers of organ damage in sera (Supplemental Figure 1B) and increased inflammation and necrosis in livers and spleens (Supplemental Figure 1, C–E), phenotypes that were rescued in *Irgm1*$^{-/-}$*Ifnar*$^{-/-}$ mice. Increased cell death in *Irgm1*$^{-/-}$ livers and spleens was dependent on IFN-I signaling (Figure 1, B and C, and Supplemental Figure 1, F and G). Compared with that in WT and *Irgm1*$^{-/-}$*Ifnar*$^{-/-}$ organs, there was increased *L. monocytogenes* growth in *Irgm1*$^{-/-}$ organs (Supplemental Figure 1, H–J). Increased growth was seen by 4 hours after infection in the peritoneum (Figure 1D), the site of *L. monocytogenes* inoculation in our model, indicating that IFN-I suppresses clearance of *L. monocytogenes* upon initial encounter. Indeed, *Irgm1*$^{-/-}$ F4/80^{hi} peritoneal macrophages internalized *L. monocytogenes* normally in vitro (Supplemental Figure 2A) but had reduced killing capacity (Figure 1E). This was associated with decreased lysosomal delivery of *L. monocytogenes* (Figure 1F and Supplemental Figure 2B), despite normal lysosomal mass (Supplemental Figure 2C) and pH (data not shown) in *Irgm1*$^{-/-}$ macrophages. *L. monocytogenes*–challenged *Irgm1*$^{-/-}$ F4/80^{hi} peritoneal macrophages also had higher expression levels of STAT1, STAT2, (Y701-)PO_4-STAT1, and (Y689-)PO_4-STAT2 than their WT and *Irgm1*$^{-/-}$*Ifnar*$^{-/-}$ counterparts (data not shown). In vivo, 4 hours after infection by GFP-expressing *L. monocytogenes*, only *Irgm1*$^{-/-}$ F4/80^{hi} macrophages showed increased bacterial load (Figure 1G and Supplemental Figure 2D).

Given that IFN-I may induce cell death (3), we examined peritoneal myeloid cells for viability (Supplemental Figure 2E). Lytic death was increased in the *Irgm1*$^{-/-}$ peritoneum on days 1 and 3 after infection and was IFN-I–dependent (Supplemental Figure 3A). Fewer neutrophils were recruited by 4 hours after *L. monocytogenes* infection to *Irgm1*$^{-/-}$ peritonea, but neutrophil accumulation increased dramatically after 24 hours in an IFN-I–dependent manner (Figure 1H), and increased citrullinated histones, a marker of lytic neutrophil death by NETosis, were detected on day 3 (Supplemental Figure 3B). Increased IFN-I–dependent lytic death was also observed among F4/80^{hi} macrophages (Supplemental Figure 3A), perhaps explaining their depletion 24 hours after infection (Figure 1, I and J). Notably, increased staining of phosphorylated mixed lineage kinase domain–like pseudokinase, a necroptosis effector, was observed only in *Irgm1*$^{-/-}$ macrophages (Supplemental Figure 3, C and D). Thus, IFN-I promotes multiple modes of proinflammatory lytic cell death in *Irgm1*$^{-/-}$ mice. Accordingly, *Irgm1*$^{-/-}$ peritoneal fluid exhibited an IFN-I–dependent increase in lactate dehydrogenase activity and proinflammatory cytokines (Supplemental Figure 3, E and F).

During peritonitis, death of resident macrophages leads to recruitment and reprogramming of Ly6C^{hi}F4/80^{-} monocytes into Ly6C^{-} F4/80^{hi} macrophages, often through an MHCII^{+}F4/80$^{lo/int}$ intermediate (5). We observed emergence of a small F4/80^{+} population on day 3 after *L. monocytogenes* infection (Supplemental Figure 2E). Unlike their WT, *Ifnar*$^{-/-}$, and *Irgm1*$^{-/-}$*Ifnar*$^{-/-}$ counterparts, all CD11b^{+}F4/80^{hi} macrophages in the *Irgm1*$^{-/-}$ peritoneum at day 3 after *L. monocytogenes* infection retained high Ly6C and did not express TIM4 (Supplemental Figure 4, A and B), a maturity marker of peritoneal macrophages (5). The CD11b^{+}F4/80^{lo} population in *Irgm1*$^{-/-}$ animals remained Ly6C^{hi} at day 3 and lacked a MHCII^{+} subpopulation (Supplemental Figure 4C). The receptor for colony-stimulating factor-1 (CD115), which is critical for survival and differentiation of monocytes, was repressed in *Irgm1*$^{-/-}$ Ly6C^{hi} cells in an IFN-I–dependent manner (Supplemental Figure 4C). Ly6C^{hi} monocytes were also elevated in *Irgm1*$^{-/-}$ blood and showed reduced CD115 and MHCII (Supplemental Figure 4E). These results suggest that excess IFN-I in *Irgm1*$^{-/-}$ mice impairs maturation of inflammatory Ly6C^{hi} monocytes into macrophages, possibly by repressing CD115.

To specifically examine myeloid IFN-I signaling, we infected *Irgm1*$^{-/-}$ mice lacking IFNAR1 solely in myeloid cells (*Irgm1*$^{-/-}$*LysM*:Cre^{+}*Ifnar*$^{Fx/Fx}$ mice). These mice showed decreased necrotic death of peritoneal myeloid cells, partial rescue of CD115 in

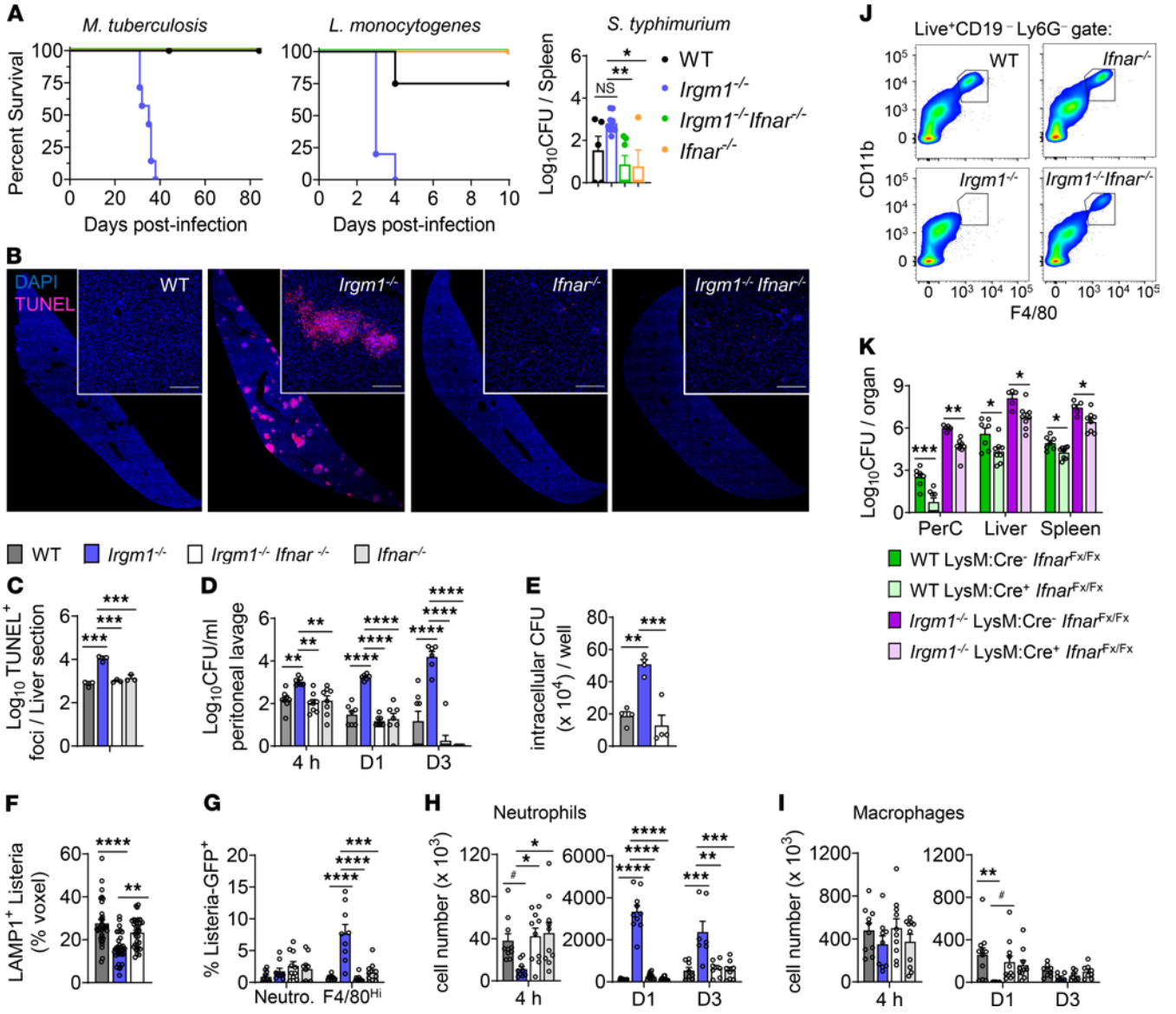

Figure 1. IFN-I induces susceptibility to bacterial infection in *Irgm1*$^{-/-}$ mice. (**A**) Survival curves after infection with *M. tuberculosis* (n = 7–10) and *L. monocytogenes* (n = 4–5). Spleen CFU on day 21 after *S. typhimurium* infection (n = 4–9). (**B**) Liver on day 3 after *L. monocytogenes* infection stained for TUNEL and DAPI. Scale bar: 200 μm. (**C**) Quantification of TUNEL$^+$ foci (n = 3). (**D**) Peritoneal lavage CFU at 4 hours, day 1, and day 3 after *L. monocytogenes* (n = 4–8). (**E**) Isolated F4/80^{hi} peritoneal macrophages exposed to *L. monocytogenes* were permeabilized for CFU count after 24 hours. (**F**) Macrophages were stained for *L. monocytogenes* and lysosome (LAMP1) at 6 hours and quantified for volumetric pixels of *L. monocytogenes* that were LAMP1$^+$ (n = 32 images). (**G**) Percentage GFP$^+$ after 4-hour infection by GFP-tagged *L. monocytogenes* (n = 9–10). (**H**) Neutrophil and (**I**) F4/80^{hi} tissue macrophage numbers in infected peritoneal lavage (n = 7–11). (**J**) Representative plot showing depletion of CD11b$^+$F4/80^{hi} macrophages at 24 hours. (**K**) CFU in peritoneal cavity (PerC), liver, and spleen on day 3 after *L. monocytogenes* (n = 5–8). Data are shown as the mean ± SEM. $^{\#}P < 0.08$, $^*P < 0.05$, $^{**}P < 0.01$, $^{***}P < 0.001$, and $^{****}P < 0.0001$ (1-way ANOVA with Tukey's adjustment for **A** and **C**–**I** or Student's t test for **K**).

CD11b$^+$F4/80^{lo}Ly6C$^-$ cells (Supplemental Figure 4, F and G), and reduced bacterial burden (Figure 1K) compared with controls, indicating that myeloid IFN-I signaling compromises myeloid cell fate and host defense in *Irgm1*$^{-/-}$ mice.

Our findings challenge the long-prevailing paradigm that IRGM1 serves as an IFN-γ–induced cell-autonomous host defense effector (1) and suggest instead that IRGM1 supports host defense by preventing excess autocrine and/or paracrine IFN-I from compromising myeloid cell fate and function. Future studies will be required to distinguish autocrine versus paracrine mechanisms.

Prashant Rai,[1] Martin Sharpe,[1] Charan K. Ganta,[2] Paul J. Baker,[3] Katrin D. Mayer-Barber,[3] Brian E. Fee,[4] Gregory A. Taylor,[4,5,6,7] and Michael B. Fessler[1]

[1]Immunity, Inflammation and Disease Laboratory and [2]Comparative & Molecular Pathogenesis Branch, National Institute of Environmental Health Sciences, NIH, Research Triangle Park, North Carolina, USA. [3]Laboratory of Clinical Immunology and Microbiology, National Institute of Allergy and Infectious Diseases, NIH, Bethesda, Maryland, USA. [4]Department of Medicine and Center for the Study of Aging and Human Development, [5]Department of Molecular Genetics and Microbiology, and [6]Department of Immunology, Duke University Medical Center, Durham, North Carolina. USA. [7]Geriatric Research Education and Clinical Center, Durham VA Health Care System, Durham, North Carolina, USA.

1. Dockterman J, Coers J. How did we get here? Insights into mechanisms of immunity-related GTPase targeting to intracellular pathogens. *Curr Opin Microbiol*. 2022;69:102189.
2. Rai P, et al. IRGM1 links mitochondrial quality control to autoimmunity. *Nat Immunol*. 2021;22(3):312–321.
3. McNab F, et al. Type I interferons in infectious disease. *Nat Rev Immunol*. 2015;15(2):87–103.
4. Matta SK, et al. *Toxoplasma gondii* effector TgIST blocks type I interferon signaling to promote infection. *Proc Natl Acad Sci U S A*. 2019;116(35):17480–17491.
5. Ardavin C, et al. Mouse tissue-resident peritoneal macrophages in homeostasis, repair, infection, and tumor metastasis. *Adv Sci (Weinh)*. 2023;10(11):e2206617.

Address correspondence to: Prashant Rai or Michael B. Fessler, National Institute of Environmental Health Sciences, 111 T.W. Alexander Drive, PO Box 12233, MD D2-01, Research Triangle Park, North Carolina 27709, USA. Phone: 984.287.4081; Email: prashant.rai@nih.gov (PR); fesslerm@niehs.nih.gov (MBF).

Conflict of interest: The authors have declared that no conflict of interest exists.

Submitted: May 3, 2023; **Accepted:** September 6, 2023; **Published:** November 1, 2023.
Reference information: *J Clin Invest*. 2023;133(21):e171982.
https://doi.org/10.1172/JCI171982.